

Supporting Information

A Ternary Composite Nanofiber-Derived Thin Membrane Electrolyte for Solid-State Li Metal Batteries

Xiaoqi Gong,^{a†} Yaozheng Pan,^{a†} Linfeng Zhong,^a Jiasheng Wang,^b Fujie Liu,^c Guangsheng Qi,^b Jing Li,^d Cong Liu^{*a} and Dingshan Yu^{*a}

- a. Key Laboratory for Polymeric Composite and Functional Materials of Ministry of Education, Key Laboratory of High-Performance Polymer-based Composites of Guangdong Province, School of Chemistry, Sun Yat-sen University, Guangzhou 510006, China.
- b. Guangzhou Lushan New Materials Co., Ltd, Guangzhou, China.
- c. School of Chemistry and Chemical Engineering, Guangxi Minzu University, Nanning, 530006, China.
- d. School of Chemical Engineering and Light Industry, Guangdong University of Technology, Guangzhou, China.

* Corresponding author

Email addresses: liuc63@mail2.sysu.edu.cn (Cong Liu), yudings@mail.sysu.edu.cn (Dingshan Yu),

† These authors contributed equally to this work.

Experimental section

Preparation of h-BN fillers

In typical, 1 g of h-BN was dispersed in 200 mL of N, N-dimethylformamide (DMF) and sonicated for 8 h to obtain the dispersed solution. Subsequently, the supernatant was carefully poured into a separate beaker, leaving behind the bulk h-BN at the bottom. The resulting supernatant was centrifuged at 5000 rpm to collect the white detached h-BN nanosheets. Finally, the h-BN products were washed with deionized water and dried overnight at 80°C.

Preparation of solid-state electrolytes

The electrospinning technique was employed for the fabrication of Poly(vinylidene fluoride-co-hexafluoropropylene) (PVH) skeleton. The electrospinning process entailed the preparation of a solution, in which 1.5 grams of PVH nanoparticles were dissolved in 10 g of DMF/acetone (7:3, v: v) and stirred for a period of 2 h at 60°C. The electrospinning solution was extruded and drawn through a syringe under high-voltage static electricity with a speed of 1 mL h⁻¹ and a voltage of 24 kV. The resulting PVH membrane was subjected to vacuum drying at 60°C for 4 h to remove the residual solvent, which was then stored for later use. A specific mass of polyethylene oxide (PEO) and LiTFSI (with a molar ratio of EO: Li⁺ of 18:1) was added to anhydrous acetonitrile, which was then stirred at 55°C for 6 h to achieve a uniform dispersion. Subsequently, h-BN with varying mass fractions were added to the mixture, which was then subjected to continuous stirring for a further two hours. The prepared solution was poured onto the PVH substrate and vacuum dried at 55°C for 36 h to completely remove the acetonitrile solvent. The solid-state electrolytes with varying h-BN contents are designated as PEO, PEO/PVH, 0.2%h-BN@PEO/PVH, 0.4%h-BN@PEO/PVH, and 0.8%h-BN@PEO/PVH electrolytes, respectively.

Materials Characterizations

Fourier transform infrared (FTIR) spectra were recorded via a FT-IR spectrometer (Thermo Nicolet Nexus 670). The crystalline structure of samples was investigated on X-

ray diffraction analysis (XRD, Rigaku Ultima IV) with Cu K α radiation (40 kV / 30 mA, $\lambda = 0.154$ nm). The morphologies were characterized by Scanning electron microscopy (SEM, Hitachi S-4800) and Transmission electron microscopy (TEM, JEM-2010 HR). The X-ray photoelectron spectra (XPS) of samples were performed on a ESCALAB 250 photoelectron spectrometer (Thermo Fisher Scientific). The atomic force microscopy (AFM) examinations were conducted on Bruker Anasys nanoIR2-fs instrument. Nanoindentation technique (Fischer Scope, ST200) was applied to mimic the punctuation of Li dendrites at nanoscale. The tensile strength of the solid-state electrolytes was inspected using the universal testing machine (CMT6103, SANS).

Electrochemical tests

An electrochemical test was conducted at 60 °C utilizing a coin cell comprising a Li-metal anode, the solid-state electrolyte and LiFePO₄ cathode. The high-loading LFP/LCO/NCM523 cathodes were fabricated by casting the slurry containing active material (80 mg), carbon black (10 mg), and PVDF (10 mg) with a high areal-loading of ~ 2 mg cm⁻² on the Al foil. After drying at 60°C overnight, the electrode was cut into round discs with a diameter of 12 mm prior to use.

The ionic conductivity of the prepared solid-state electrolytes was determined by EIS technique using a symmetric coin cell with two stainless steel electrodes. The cells were performed with the frequency range from 10⁻² to 10⁵ Hz and a voltage amplitude of 10 mV. The ionic conductivity (σ) of the electrolyte was calculated using below equation, where R_b is the resistance (Ω), L represents the thickness (cm), and S stands for the area of the solid electrolyte (cm²):

$$\sigma = \frac{L}{R_b S}$$

The Li-ion transference number (t_{Li^+}) of the solid-state electrolytes was measured in a symmetrical Li//Li cell. A voltage of 10 mV (ΔV) was applied and EIS spectra of the cell before and after polarization were obtained from 10⁻² to 10⁵ Hz. The Li-ion transference number was determined based on the following equation:

$$t_{Li^+} = \frac{I_s(\Delta V - I_i R_i)}{I_i(\Delta V - I_s R_s)}$$

Where t_{Li^+} , I_s , I_i , R_s and R_i are the Li-ion transference number, the current and the resistance at the final state and initial state, respectively.

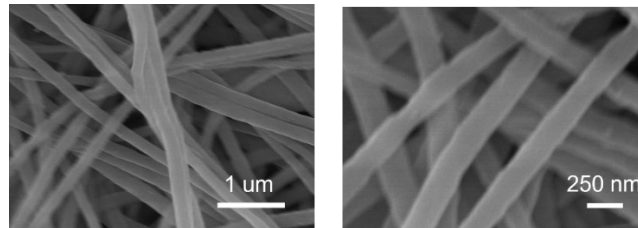


Fig. S1 SEM images of PVH membrane of different sizes.

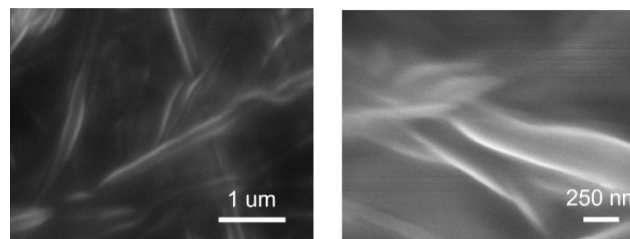


Fig. S2 SEM images of the h-BN@PEO/PVH electrolyte of different sizes.

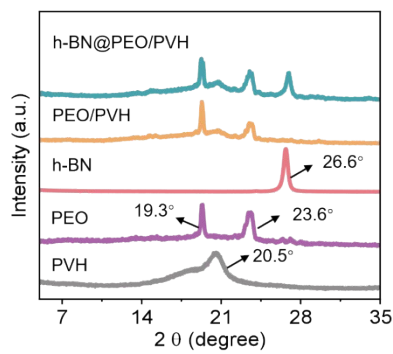


Fig. S3 XRD patterns of h-BN fillers, PVH substrate, PEO, PEO/PVH and h-BN@PEO/PVH electrolytes.

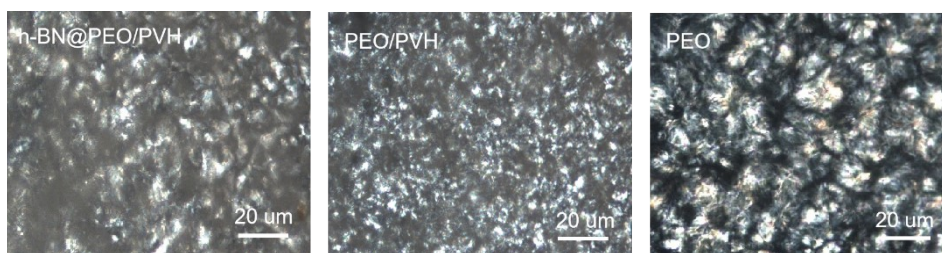


Fig. S3 Polarization microscopies of h-BN@PEO/PVH, PEO/PVH and PEO electrolytes.

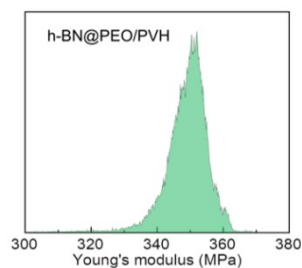


Fig. S4 The distribution curve of Young's modulus collected from AFM image of h-BN@PEO/PVH electrolyte.

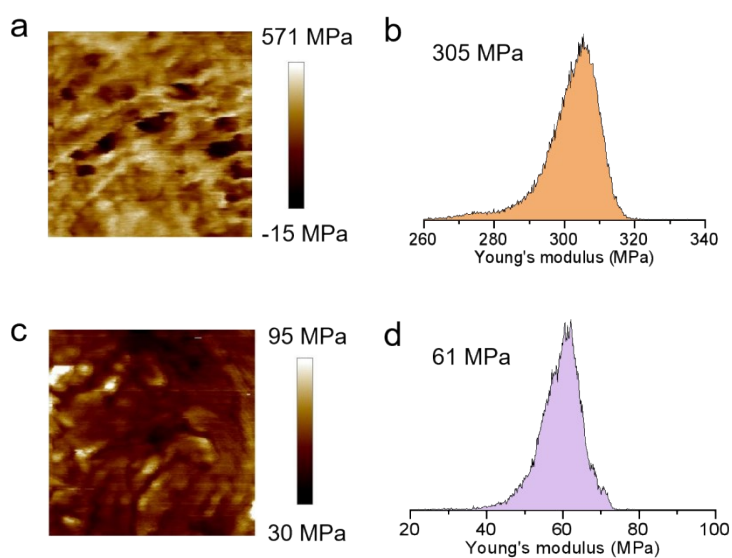


Fig. S5 AFM images of Young's modulus and their distribution curves of (a, b) PEO/PVH and (c, d) PEO electrolytes.

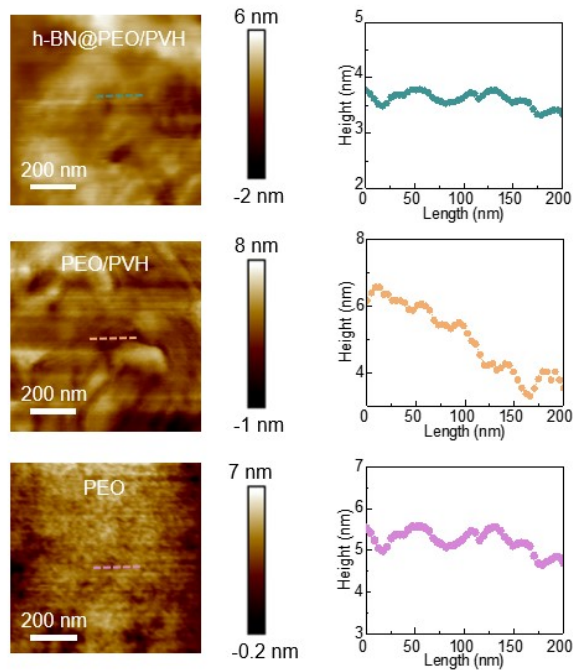


Fig. S6 AFM images of the surface roughness on different electrolytes.

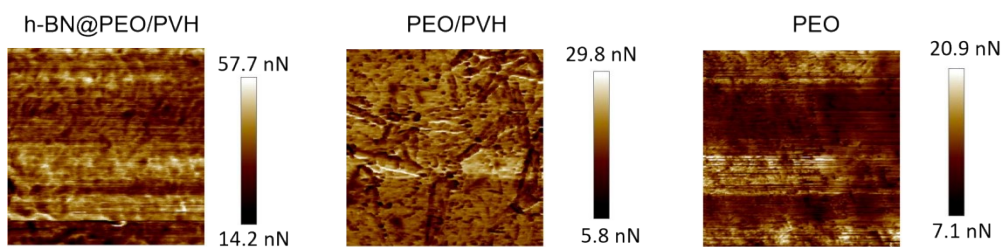


Fig. S7 AFM images of the adhesion force on different electrolytes.

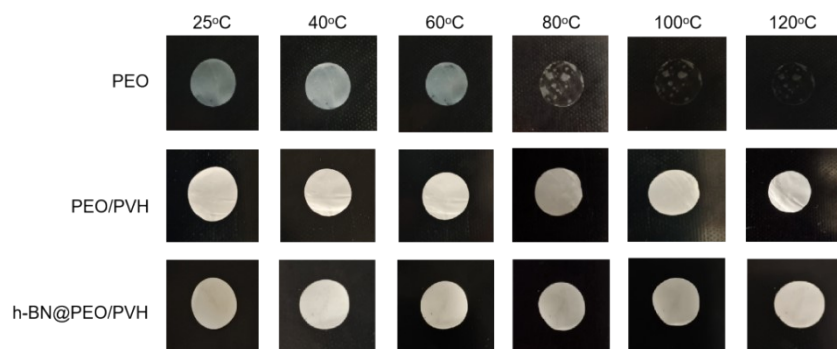


Fig. S8 The thermal stability of PEO, PEO/PVH and h-BN@PEO/PVH electrolytes at different temperatures.

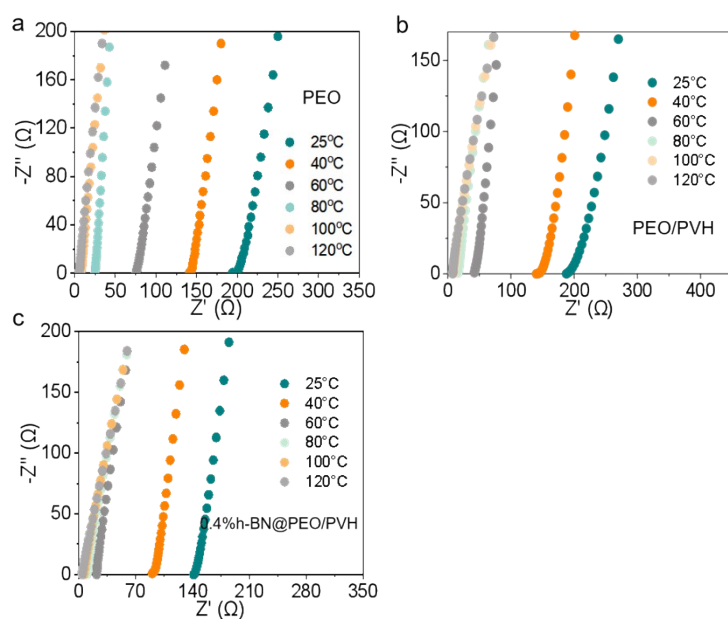


Fig. S9 EIS curves of (a) PEO, (b) PEO/PVH and (c) 0.4%h-BN@PEO/PVH electrolytes. (d) The ionic conductivity at 60 °C of PEO, PEO/PVH and 0.4%h-BN@PEO/PVH electrolytes.

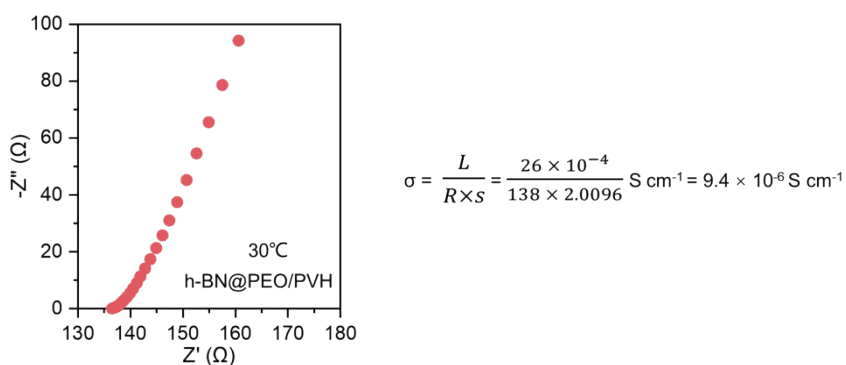


Fig. S10 The ionic conductivity of h-BN@PEO/PVH electrolytes at 30 °C.

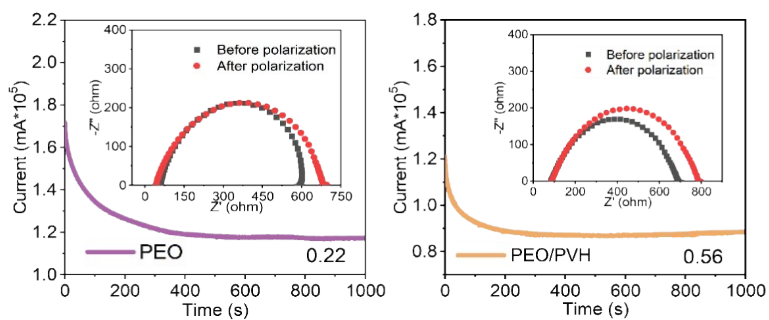


Fig. S11 Li-ion transference number of PEO and PEO/PVH electrolytes at 60 °C.

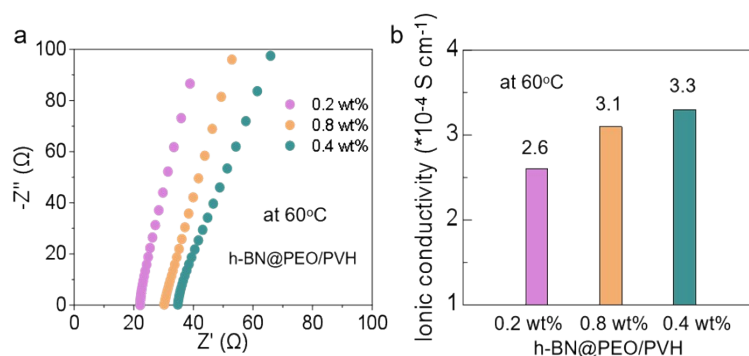


Fig. S12 (a) EIS curves and (b) the ionic conductivities at 60 °C of h-BN@PEO/PVH electrolytes with different h-BN contents.

Tab. S1 The comparison of the h-BN@PEO/PVH electrolyte with previously reported PEO-based electrolytes.

Solid electrolyte	Li-ion transference number	Filler content (wt%)	Thickness (μm)	Voltage window (V)	Ref.
h-BN@PEO/PVH	0.74 (60°C)	h-BN (0.4%)	~ 26	5.0	This work
PEO-ZCNF	0.62 (60°C)	ZCNF (10%)	~ 150	4.51	Angew. Chem. 2024, 136, e202400477.
LAZP/PEO	0.43 (60°C)	LAZP (20%)	~ 150	4.6	Inorg. Chem. Front., 2024, 11, 1289.
VCOF-PEO	0.38 (60°C)	VCOF-1 (4%)	~ 618	4.0	J. Mater. Chem. A 2024, 12, 1694.
PEO-5%C4P	0.70 (60°C)	C4P (5%)	~ 110	2.8	Adv. Mater. 2023, 2308507.
PEO/MOFs-NH ₂	0.64 (60°C)	MOFs-NH ₂ (10%)	~ 100	4.5	Adv. Mater. 2023, 2303193.
PEO-BIT-BOB HNFs	0.54 (50°C)	BIT-BOB HNFs (10%)	~ 120	4.75	Adv. Funct. Mater. 2023, 33, 2307263.
PEO-LLZO	0.41 (60°C)	LLZO (7.5%)	~ 100	5.3	ACS Appl. Mater. Interfaces 2023, 15, 38759.
PEO-SCP	0.42 (60°C)	SCP (5%)	~ 100	4.8	J. Mater. Chem. A 2022, 10, 14849.
SiO ₂ -PEO	0.42 (60°C)	SiO ₂ (10%)	~ 200	5.3	J. Mater. Chem. A 2022, 10, 3400.